SOLAR WIND EFFECTS ON GENESIS SILICON COLLECTOR SUBSTRATE STRUCTURE: OBSERVATION OF LAYERS IN TEM CROSS-SECTION

J. H. Allton.[1], L. P. Keller[1], Z. Rahman[2], C. P. Gonzalez[2], K. K. Allums[3], R. A. Synowicki[4] and A. J. G. Jurewicz[5], [1]NASA/Johnson Space Center, Mail Code XI, 2101 NASA Parkway, Houston, TX 77058, Judith.h.allton@nasa.gov, [2]Jacobs JETS, NASA/JSC, Houston, TX 77058, [3]HX5- Jacobs JETS, NASA/JSC, Houston, TX 77058, [4]J. A. Woollam Co. 645 M St., Lincoln, NE 68508, [5]ASU/CMS P.O.#6004 Tempe, AZ 85287.

Introduction: The Genesis Discovery Mission returned to Earth solar wind that was collected in passive substrates over 853 days from 2001 to 2004, in the declining phase of solar cycle 23, at Earth-Sun Lagrangian point, L1. Over 300 collectors, comprised of 9 high-purity materials, were exposed to the solar wind under 4 conditions: bulk solar wind or the individual regimes: coronal hole solar wind (CH, high speed), interstream solar wind (IS, low speed) or coronal mass ejections (CMEs). Regime samples are important for the interpretation of bulk solar wind results because each type of solar wind represents a different set of solar processes. The mission is described in [1]. The collector materials are described in [2]. Reisenfeld *et al.* [3] documented the *in situ* solar wind during the collection period, concluding that the state of the solar wind was typical of conditions over the past 4 solar cycles.

Quest to Develop a Useful Ellipsometry Model for Silicon Collectors: The pre-flight purpose of ellipsometry was for Curation to assess molecular film contamination on Genesis returned collectors. However, on flown samples, ellipsometry data was difficult to model, suggesting structural changes induced by solar wind [4, 5, 6, 7]. The current effort is to investigate silicon surface oxide formation from aging and from handling (e.g., cleaning, analysis, etc). The intent is to define the parameters needed for ellipsometry models. That is, obtaining thicknesses and characteristics of surface layers to be modeled, from TEM cross-sections of typical collectors. Keller and Rahman produced a TEM cross-section of sample 61202, a bulk solar wind in Czochralski silicon (Fig. 1).

In the associated EDX element maps (Fig. 2) chemistry can be correlated with features in the TEM image. A thin native oxide layer is visible on the O map at the solar wind collection surface. The distinct amorphous silicon (α-Si) layer (layer 3 in Fig. 1) extending 15-16 nm below the surface appears less intense on the silicon element map (less dense?) than the strained crystalline silicon below.

TEM cross-sectional observations are also planned for the individual solar wind regimes. The TEM and EDX results from cross-sections of coronal hole, interstream and coronal mass ejection regime samples will likely show differences relatable to fluence and velocity distributions of the solar wind samples; e.g., the thickness of the α-Si and the zone of strained silicon. Any differences in thickness of these layers can be inter-compared directly because the silicon substrates form a standardized set comprised of pure CZ single crystal orientation 1-0-0.

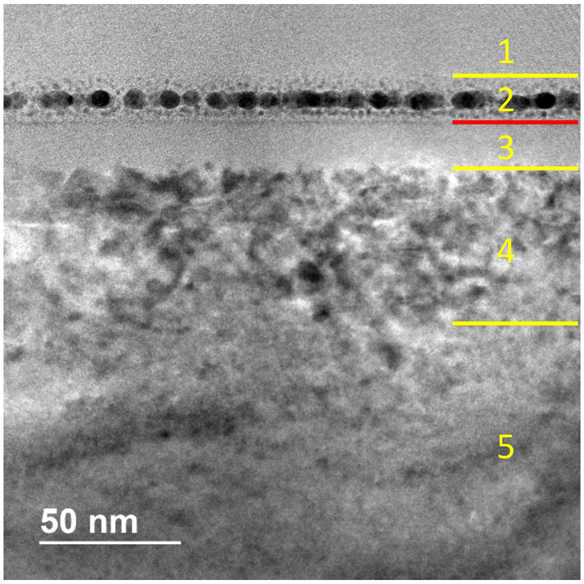

Fig. 1. TEM cross-section of CZ bulk solar wind sample 61202. Red line marks solar wind surface. Layer 2 is thin platinum marker (5-10 nm). Layer 1 is a protective carbon strap. Layer 3 α-Si (15-16 nm). Layer 4 strained silicon crystal (55-60 nm). Layer 5 crystalline silicon (confirmed by XRD).

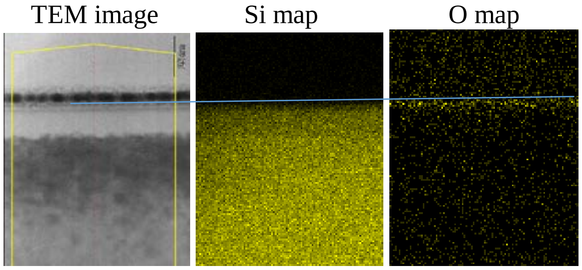

Fig. 2. Energy dispersive X-ray maps from FIB section. Light blue line marks bottom of Pt layer.

***In situ* Solar Wind Measurements**: [3] discusses *in situ* solar wind measurements taken during the Genesis collection period from (1) the onboard Genesis Ion

Monitor (GIM) and (2) the Solar Wind Ion Composition Spectrometer (SWICS) onboard the Advanced Composition Explorer (ACE), a spacecraft located at a similar distance from the Sun in the ecliptic. GIM monitored H and He; SWICS gave a broader characterization of the solar wind, including heavy ion data. Results from [3] for solar wind H and He fluences are in Table 1. Fig. 3 compares regime H-ion fluence and velocity distributions. Damage to the substrate can be calculated for SW ion implantation by relating velocity to impact energy (i.e., $E=1/2mv^2$). Between CME and bulk regimes there is a 5-fold increase in H fluence and a similar peak position, for example, if one wanted to compare amorphization with H fluence.

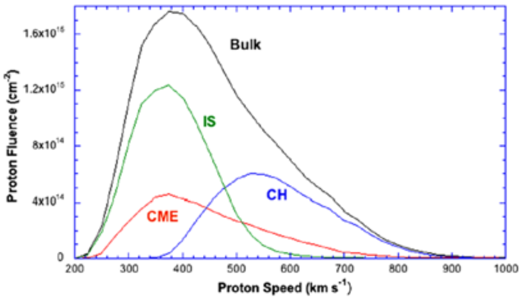

Fig. 3. Proton speed vs fluence measured by GIM [3].

What's next? Curation plans to monitor oxide formation with aging (and sample handling/use) in silicon using ellipsometry models based upon the layer thickness and structural information from TEM cross-sections. There may be other uses as well. Calaway et al. [7] identified α-Si in a fragment welded to a Genesis B/C collector, but did not see a continuous amorphous layer in the primary substrate. That earlier fragment may have been anomalous (e.g. partially shielded from SW by the wall of the cannister's lid) so that there wasn't enough damage for the α-Si to form. Alternatively, α-Si may either form intermittently, the layer of α-Si may form over time. These or other mechanisms can be investigated by re-analysis of the samples from [7]. Titov et al. [9] discusses formation of α-Si from ion-implant damage and found that it begins below the oxide layer and requires a threshold fluence. Although α-Si growth may stimulate radiation induced segregation (e.g., [10]) which may or may not effect SW retention [11], it may also protect SW in the collectors. For example, Paramasivan *et al.* [12] found that aggressive cleaning removed significantly less silicon than expected from a Si collector, and that lower etch rate seemed to be related to the SW H. If the α-Si layer is only intermittently present, better ellipsometry models may eventually allow Curation to identify fragments having an α-Si layer at a PI's request.

Thickness (and presence or absence) of layers observed in regime samples can be compared with those measured in Fig. 1. Using this unique database of standard silicon substrates irradiated by known fluence, velocity and particle composition, Genesis PI's can begin to fully characterize the physical and chemical changes that solar wind collection produced in silicon collectors.

Ellipsometry modeling will eventually include additional cross-sections of other materials such as sapphire and silicon on sapphire. As yet, we know little about the structural changes solar wind collection has on these materials and how they will effect solar wind measurement. We do know, by observation, that flight silicon on sapphire has very different chemical properties than non-flight material [13]. So, in addition to aiding ellipsometry, a database of TEM sections of non-silicate Genesis collectors should give both Genesis Curation and individual PIs information they need to handle and analyze these precious samples in the most efficient and non-destructive manner.

References:

[1] Burnett, D. S. et al. (2003) *Space Sci. Rev.*, **105**, 509-534. [2] Jurewicz A. J. G. *et al.* (2003) *Space Sci. Rev.*, **105**, 535-560. [3] Reisenfeld, D. B. (2013) Space Sci. Rev. [4] McNamara K. M. and Stansbery E. K. (2005) *LPSC XXXVI*, #2402. [5] Stansbery E. K. and McNamara K. M.(2005) *LPSC XXXVI*, #2145. [6] Calaway, M. J. et al (2006) LPSC XXXVII. #1420. [7] Calaway, M. J. et al (2007) LPSC XXXVIII. #1632. [8] Heber, V. S. *et al.* (2012) Astrophys. J., v. 759/121. [9] Titov, A. I. *et al.* (2003) Semiconductors **37**(3), 340-346. [10] King, B. *et al.* (2008) Appl. Surf. Sci., 255, 1455-1457. [11] Jurewicz A. J. G. *et al.* this meeting. [12] Paramasivan G. J. *et al.* (2018) *LPSC XLIX*, #2886. [13] Humayun M. (2011) *LPS XLVII*, Abstract #1211.

Table 1 H and He fluences (~98% of the solar wind) by regime, comparing GIM, ACE and sample analysis

Regime	Duration, days	GIM H Fluence X10^{15}cm^{-2}	ACE H Fluence X10^{15}cm^{-2}	GIM He Fluence X10^{14}cm^{-2}	ACE He Fluence X10^{14}cm^{-2}	Sample analysis[8] He Fluence X10^{14}cm^{-2}
Bulk	853	20.6	21.3	8.09	8.58	8.29
IS	334	9.15	9.35	3.19	4.08	3.15
CH	313	6.40	6.33	2.52	2.12	2.57
CME	193	4.73	5.26	2.26	2.26	2.53